Check for updates

Fast and safe synthesis of micron germanium in an ammonia atmosphere using Mo_2N as catalyst

Baojun Ma, [ID] * Dekang Li, Xiaoyan Wang and Keying Lin

Here, we reported a new method for fast and safe synthesis of a micron germanium (Ge) semiconductor. The Ge was successfully prepared from mixed GeO_2 with a low amount of MoO_3 by the NH_3 reduction method at 800 °C for an ultra-short time of 10 min. XRD patterns show that the Ge has a tetragonal structure. SEM images show that the size of the Ge particles is from 5 μm to 10 μm, and so it is on the micron scale. UV-visible diffuse reflectance spectroscopy shows that the Ge has good light absorption both in the ultraviolet and visible regions. The formation of Ge mainly goes through a two-step conversion in the NH_3 flow. Firstly, GeO_2 is converted to Ge_3N_4, and then Ge_3N_4 is decomposed to generate Ge. The comparison experiments of MoO_3 and Mo_2N demonstrate that Mo_2N is the catalyst for the Ge synthesis which improves the Ge_3N_4 decomposition. The presented fast and safe synthesis method of Ge has great potential for industrialization and the proposed Mo_2N boosting the Ge_3N_4 decomposition has provided significant guidance for other nitride decomposition systems.

1 Introduction

With the development of advanced electronic information industries, semiconductor materials have attracted widespread attention due to their unique optical and electrical properties.[1–6] Ge as an important semiconductor material with stable chemical properties and obvious non-metallic properties has many advantages, such as non-toxicity, biocompatibility, electrochemical stability, current microelectronics compatibility, *etc.*[7–13] At present, Ge has extensive and important applications in fields such as semiconductors, aerospace measurement and control, nuclear physics detection, optical fiber communication, infrared optics, solar cells, chemical catalysts, and biomedicine.[14–20] Ge is one of the most dispersed elements and there is almost no concentrated Ge deposit in the Earth's crust. Thus, it is particularly important to find suitable methods to enrich, prepare and purify Ge.

The synthetic method of Ge can be divided into physical and chemical methods. The physical methods mainly include chemical vapor deposition,[21] gas phase pyrolysis,[22] plasma technology,[23–25] sputtering,[26,27] etching,[28,29] laser ablation[30] and so on. However, these technological processes need extreme temperatures and pressures and are expensive. Chemical methods mainly include room temperature reduction of a $GeCl_4/Br_4$ precursor,[31,32] high temperature reduction of a GeI_2/I_4 precursor,[33,34] a one-step synthesis method,[35,36] an electrodeposition method[37–41] and so on. In the industry, rough Ge is commonly prepared by the reduction of GeO_2 in hydrogen flow at 650–680 °C, and then Ge with high purity is obtained by chemical gasification and decomposition of rough Ge. However, in the process of preparing rough Ge, the produced hydrogen is a dangerous gas due to its large range of the explosion limit. In addition, a leak of hydrogen is not easy to discover due to it being colorless and tasteless. So, it is necessary to develop and improve a safe and low-cost method to produce rough Ge.

Ammonia is an important chemical raw material, which has important applications in industrial and agricultural production. At the same time, ammonia is also a reducing gas capable of reducing various metal oxides.[42–45] Here, we successfully prepared micron Ge material in ammonia atmosphere using GeO_2 as raw material with some MoO_3 in 10 min. The transformation process from GeO_2 to Ge and the molybdenum based catalyst were determined. The synthesis method of Ge has the advantages of safe, fast and low cost, which is beneficial to industrial production.

2 Experimental

2.1 Synthesis of Ge

All the chemical agents are from China National Pharmaceutical Group Corporation. GeO_2 as raw material and a small amount of MoO_3 are mixed and milled in a mortar for 30 minutes. The mixed samples are the calcined in an ammonia flow of 100 mL min^{-1} at different temperature and for different time. The synthesis of Ge in H_2 flow is same as that in NH_3 flow except H_2 instead of NH_3.

Also, in this paper A/B means A mixed with B. For example, Mo_2N/GeO_2 means Mo_2N mixed with GeO_2.

State Key Laboratory of High-efficiency Coal Utilization and Green Chemical Engineering, College of Chemistry and Chemical Engineering, Ningxia University, Yinchuan, 750021, People's Republic of China. E-mail: bjma@nxu.edu.cn

2.2 Characterization

The structure of the as-prepared Ge was determined by X-ray diffraction (D/MAX2500, Rigaku, Japan) with a Cu-K$_\alpha$ radiation at a voltage of 4 kV at room temperature. The ultraviolet-visible diffuse reflectance spectra (UV-vis DRS) were obtained on a spectrometer (U-4100), and BaSO$_4$ was used for the corrected base line. The size and morphology were examined by scanning electron microscopy (SEM, JSM7500F) with the accelerating voltage of 0.5–30 kV and transmission electron microscopy (TEM, F20) with the accelerating voltage of 120 kV.

3 Results and discussion

3.1 Synthesis of Ge in NH$_3$ flow using Mo based catalyst

Fig. 1 shows the XRD patterns of GeO$_2$ calcined at different temperatures in an ammonia atmosphere. The XRD of the GeO$_2$ is also present for comparison. When the reaction temperature is lower than 800 °C, GeO$_2$ (PDF # 36-1463) still remain unchanged. At 800 °C, all GeO$_2$ changed into Ge$_3$N$_4$ (PDF # 38-1374). At 900 °C, a part of Ge (PDF # 04-0545, $2\theta = 27.5°$) generates which indicates a small part of Ge$_3$N$_4$ decomposes at overhigh temperature.

Fig. 2 shows the XRD patterns of 5.0 wt% MoO$_3$/GeO$_2$ calcined in NH$_3$ flow at different temperatures for 2 h. It can be seen that when the reaction temperature is at or above 800 °C, almost all the GeO$_2$ are changed into Ge (PDF # 04-0545). Comparing with Fig. 1, the introduction of the Mo element decreases the reaction temperature of Ge generation over 100 °C.

Fig. 3 shows XRD patterns of 5.0 wt% MoO$_3$/GeO$_2$ calcined in NH$_3$ flow at 800 °C for different time. The process of Ge generation is ultra fast and almost all the GeO$_2$ can be reduced to Ge in 10 min. Fig. 4 shows the XRD pattern of MoO$_3$/GeO$_2$ with different mass ratio calcined in ammonia flow. When the amount of MoO$_3$ is less than 5.0%, the reaction product is Ge and Ge$_3$N$_4$ (e.g. the sample of 2.0 wt% MoO$_3$/GeO$_2$). When the amount of MoO$_3$ is 5.0%, almost all the GeO$_2$ is converted to Ge. In view of the fact of that GeO$_2$ changed into Ge$_3$N$_4$ (Fig. 1, 800
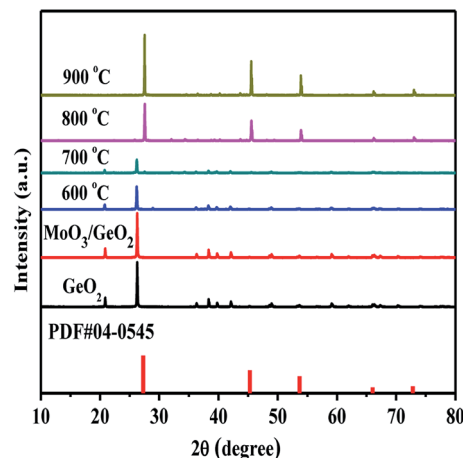

Fig. 2 XRD patterns of commercial GeO$_2$ and samples of 5.0 wt% MoO$_3$/GeO$_2$ calcined in NH$_3$ flow at different temperatures for 2 h.
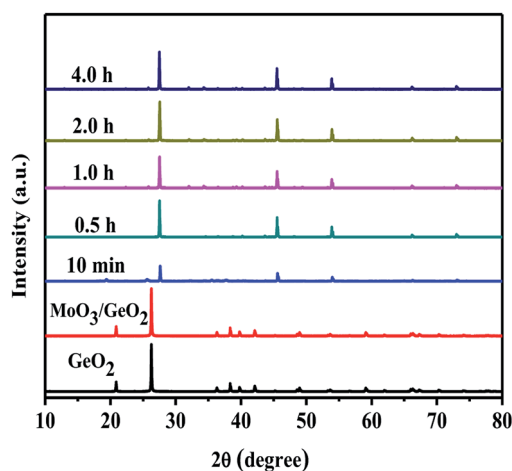

Fig. 3 XRD patterns of commercial GeO$_2$, 5.0 wt% MoO$_3$/GeO$_2$ and 5.0 wt% MoO$_3$/GeO$_2$ calcined in NH$_3$ flow at 800 °C for different time.
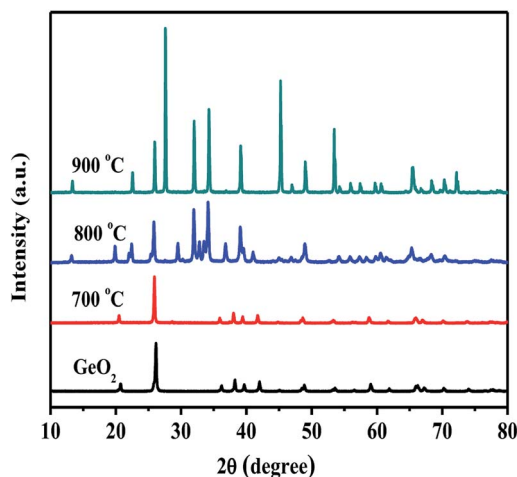

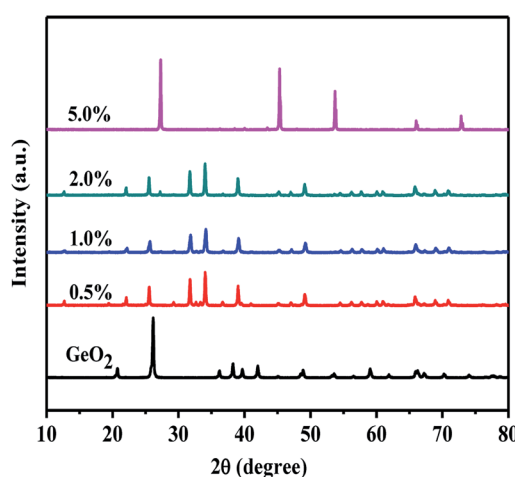Fig. 1 XRD patterns of commercial GeO$_2$ and GeO$_2$ calcined in NH$_3$ flow at different temperatures for 2 h.

Fig. 4 XRD patterns of GeO$_2$ and MoO$_3$/GeO$_2$ with different MoO$_3$ loading mass ratio calcined in NH$_3$ flow at 800 °C for 0.5 h.

°C) without any catalyst, we inferred the process Ge generation is that first the GeO_2 transfers into Ge_3N_4, and then the Ge_3N_4 decomposes into Ge with the Mo base catalyst. This ultra fast method of Ge generation using Mo based catalyst has major advantages of low cost and high efficiency.

3.2 Determination of the catalyst of Ge generation

It is well known the molybdenum oxide will change into molybdenum nitride in NH_3 atmosphere at high temperature. So, it is necessary to judge which Mo species play the catalytic role in the Ge generation. Fig. 5 shows XRD patterns of MoO_3 calcined in the NH_3 flow at different temperatures. At 600 °C, some MoO_3 (PDF # 35-0609) is reduced into MoO_2 (PDF # 32-0671). When the temperatures reach at and above 700 °C, all MoO_3 is converted to Mo_2N (PDF # 25-1366). In Fig. 2, Ge is generated at 800 °C from MoO_3/GeO_2. At this moment (800 °C), the MoO_3 had been reduced into Mo_2N (Fig. 5, 800 °C), and the GeO_2 had been reduced into Ge_3N_4 (Fig. 1, 800 °C). These results indicate that the Mo_2N generated by MoO_3 acts as a catalyst and improves the decomposition of the Ge_3N_4 into Ge.

In order further determine the origination (Mo_2N or MoO_3) of the catalysis role in Ge generation, the calcination experiments in nitrogen flow using GeO_2 and Ge_3N_4 as raw materials have been designed. Fig. 6 shows the XRD patterns of Mo_2N/GeO_2, MoO_3/GeO_2, Mo_2N/Ge_3N_4 and MoO_3/Ge_3N_4 calcined in N_2 atmosphere at 800 °C for 2 h. It can be seen that there are all a small amount of Ge generated by the addition of Mo_2N whether the raw material is GeO_2 or Ge_3N_4. However, by the addition of MoO_3, there is no Ge generation for both MoO_3/GeO_2 and MoO_3/Ge_3N_4. These again demonstrate that Mo_2N plays the catalysis role in Ge generation, whereas MoO_3 is not the catalyst.

3.3 Comparison with the industrial preparation method of Ge in H_2 flow

In order to compare our preparation method with industrial method, GeO_2 is reduced into Ge in hydrogen atmosphere has been carried out. Fig. 7 shows the XRD patterns of GeO_2 calcined in hydrogen flow at different temperatures for 4 hours. At or over 500 °C, Ge is generated in H_2 flow, and 650 °C is
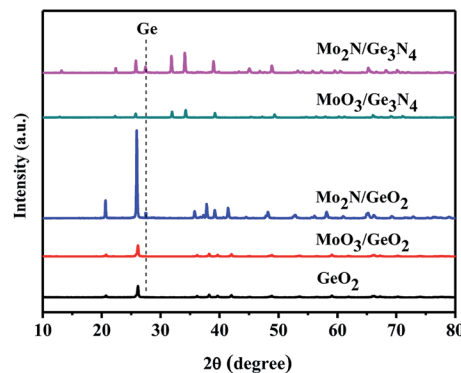

Fig. 6 XRD patterns of GeO_2, 5.0% Mo_2N/GeO_2, 5.0% MoO_3/GeO_2, 5.0% Mo_2N/Ge_3N_4 and 5.0% MoO_3/Ge_3N_4 calcined in N_2 atmosphere at 800 °C for 2 h.
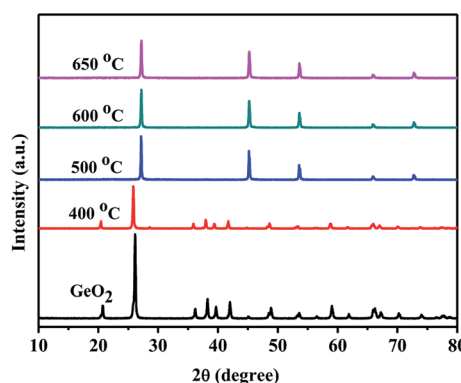

Fig. 7 XRD patterns of GeO_2 calcined in hydrogen atmosphere at different temperatures for 4 h.

chosen generally in the industry. Fig. 8 shows the XRD pattern of GeO_2 calcined in hydrogen flow at 500 °C for different time. Ge can be produced in the H_2 flow in 2 hours. So, compared with the industrial method in the H_2 flow, our preparation method in the NH_3 flow with Mo_2N catalyst has the advantages of ultra short reaction time (10 min vs. 2 h) and more safety (NH_3 vs. H_2), though the reaction temperature is higher (800 °C
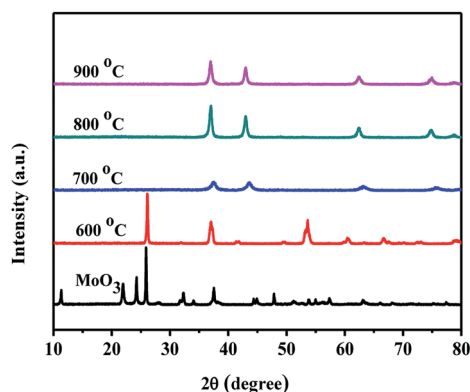

Fig. 5 XRD patterns of MoO_3 and MoO_3 calcined in NH_3 flow at different temperatures for 2 h.
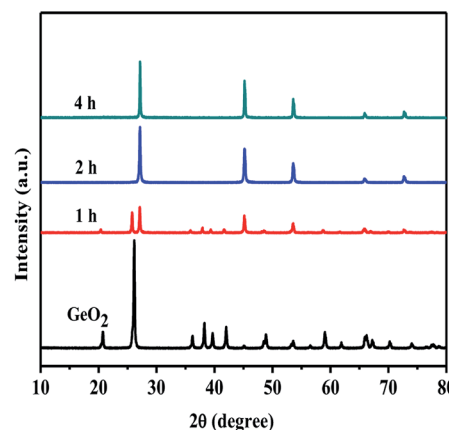

Fig. 8 XRD patterns of GeO_2 calcined in H_2 flow at 500 °C for different time.

vs. 650 °C). We also performed the experiment which the GeO_2 was calcined in H_2 flow at 800 °C for the further contrast. The Fig. 9 shows the XRD pattern of GeO_2 calcined in hydrogen flow at 800 °C for different time. The GeO_2 was converted into Ge in 10 min under the hydrogen atmosphere at 800 °C. It is similar to that of in the NH_3 flow reduction. However, calcining GeO_2 in an ammonia atmosphere means more secure.

3.4 The physical properties of prepared Ge

Fig. 10 shows the morphologies of the raw material GeO_2 and the prepared Ge in NH_3 flow with different magnifications. The GeO_2 particles (Fig. 10a–c) are uniform and show sharp angular shapes. The prepared Ge in NH_3 flow (Fig. 10d–f) shows a smooth surface and some agglomeration, indicating the structure changes from GeO_2 to Ge. The size of Ge is between 5 μm and 10 μm. Fig. 11 shows the HRTEM of prepared Ge in NH_3 flow, the lattice fringes of Ge with interplanar distances of 0.237 nm is indexed to the (111) planes of Ge.

In order to further explore the morphology changes in the formation process of Ge, SEM as shown in Fig. 12 has been carried out for the samples prepared from MoO_3/GeO_2 for different times and with different MoO_3 mass ratios. Compared the Fig. 12b with Fig. 12a, it is found the rod-shaped material
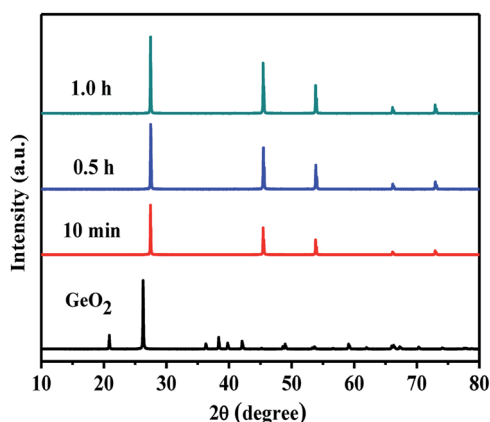

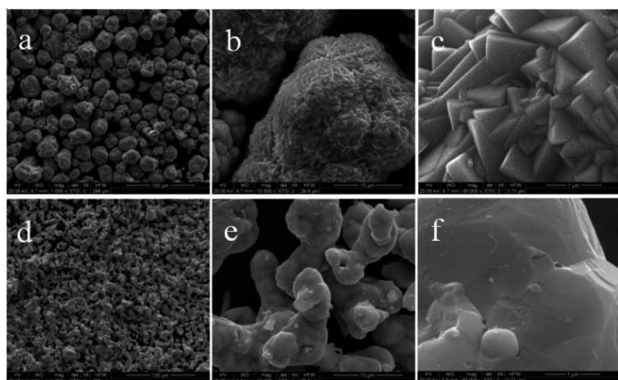**Fig. 9** XRD patterns of GeO_2 calcined in H_2 flow at 800 °C for different time.

Fig. 10 SEM images of the raw material of GeO_2 (a–c) and the Ge (d–f) prepared from 5% MoO_3/GeO_2 in NH_3 flow at 800 °C for 2 h.
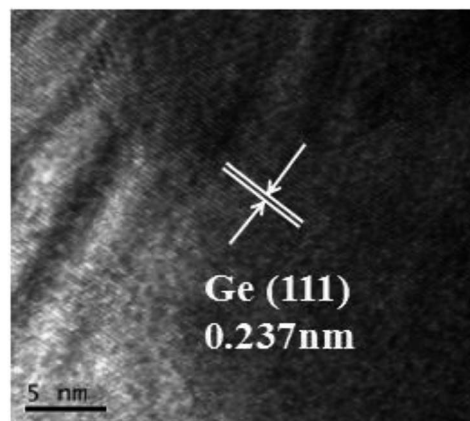

Fig. 11 HRTEM of Ge prepared in the NH_3 flow from GeO_2 mixed with 5.0% MoO_3 at 800 °C for 2 h.

(Fig. 12a) decreases and the large smooth-surfaced Ge (Fig. 12b) increases with the reaction time prolonging. Associate with XRD patterns in Fig. 4, the rod-shaped material can be inferred as Ge_3N_4. Compared the Fig. 12c with Fig. 12b, it can be seen that there is hardly any Ge_3N_4 particles in the Fig. 12c, indicating that almost all Ge_3N_4 transforms into Ge with the increase of MoO_3. Here, the MoO_3 had been converted into Mo_2N due to in the NH_3 flow at 800 °C (Fig. 5, 800 °C). Fig. 12 again demonstrates the process of Ge generation goes through two stages. Firstly, GeO_2 is reduced to Ge_3N_4, and then Ge_3N_4 decomposed into Ge by the catalysis of Mo_2N.

Fig. 13 shows the UV-vis diffuse reflectance spectra of MoO_3/GeO_2 calcined in the NH_3 flow with different mass ratios of MoO_3. The raw material of GeO_2 show a strong light absorption at ultraviolet region with the absorption edge of 218 nm, which means it is a large gap semiconductor. With the amount of MoO_3 increasing from 0 to 5.0%, the light absorption region gradually extends from ultraviolet region to visible region and the absorption strength gradually increases. The Ge prepared from 5.0% MoO_3/GeO_2 shows the most strongest light absorption in the range from 200 nm to 800 nm. The light absorption curve of the Ge prepared in NH_3 flow is same as that prepared in H_2 flow except the absorption strength. The difference of absorption strength can be attributed to the small amount of Mo_2N catalyst.
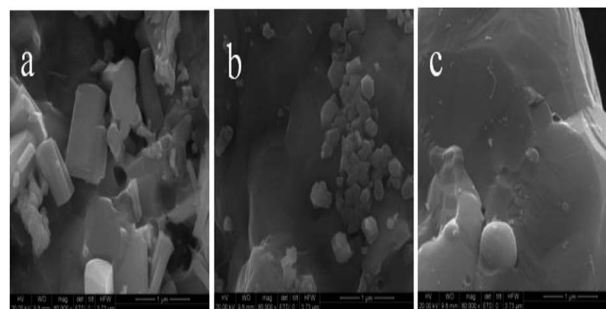

Fig. 12 SEM images of samples prepared in the NH_3 flow from 2.0% MoO_3/GeO_2 at 800 °C for 0.5 h (a), 2.0% MoO_3/GeO_2 at 800 °C for 2 h (b) 5% MoO_3/GeO_2 at 800 °C for 2 h (c).
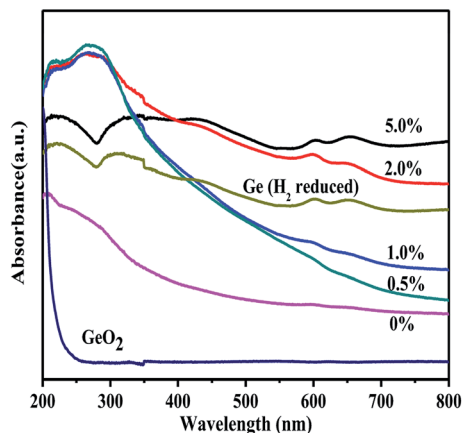
Fig. 13 The UV-visible diffuse reflectance spectra of MoO_3/GeO_2 with different mass ratios of MoO_3 calcined in NH_3 flow at 800 °C for 2 h. The spectra of GeO_2 and Ge prepared in the H_2 flow at 650 °C for 4 h are presented for comparison.

4 Conclusions

A fast, low cost and safe method for the Ge synthesis has been reported by the NH_3 reduction of GeO_2 using a Mo_2N catalyst. When GeO_2 and 5.0% MoO_3 is mixed and nitrided in NH_3 flow at 800 °C, the Ge is formed in 10 min. The prepared Ge shows micron scale particles size and good light absorption both in the ultraviolet and visible region. The reaction mechanism of Ge generation carries out a two-stage process. GeO_2 is converted into Ge_3N_4 firstly, and then Ge_3N_4 is decomposed into Ge with the Mo_2N catalyst. Mo_2N instead of MoO_3 is demonstrated the catalyst for the Ge generation by two proofs. One is that MoO_3 is converted into Mo_2N at 800 °C in the NH_3 flow. Another is that a small part of Ge is produced from both the mixed Mo_2N/GeO_2 and the Mo_2N/Ge_3N_4 calcined in N_2 flow, whereas there is no Ge generated from both MoO_3/GeO_2 and the MoO_3/Ge_3N_4. Finally, the method for Ge preparation in NH_3 flow has been compared with the industrial method in H_2 flow. Our presented method has the advantages of fast and safety and has great potential for industrialization. The proposed Mo_2N boosting the Ge_3N_4 decomposition has guiding significance to other nitride decomposition system.

Conflicts of interest

There are no conflicts to declare.

Acknowledgements

Notes and references

1 C. B. Murray, D. J. Norris and M. G. Bawendi, *J. Am. Chem. Soc.*, 1993, **115**, 8706–8715.
2 Y. Wang and N. Herron, *J. Phys. Chem.*, 1991, **95**, 525–532.
3 L. Zhang and M. Jaroniec, *Appl. Surf. Sci.*, 2017, **430**, 2–17.
4 I. D. Samuel and G. A. Turnbull, *Chem. Rev.*, 2007, **107**, 1272–1295.
5 H. A. Qayyum, M. F. Al-Kuhaili, S. M. A. Durrani, T. Hussain and S. H. A. Ahmad, *J. Alloys Compd.*, 2018, **747**, 374–384.
6 Q. Yin and C. L. Hill, *Joule*, 2017, **1**, 645–646.
7 P. Reiss, M. Carrière, C. Lincheneau, L. Vaure and S. Tamang, *Chem. Rev.*, 2016, **116**, 10731–10819.
8 A. M. Derfus, W. Chan and S. N. Bhatia, *Nano Lett.*, 2004, **4**, 11–18.
9 L. Ye, K. T. Yong, L. Liu, I. Roy, R. Hu, J. Zhu, H. Cai, W. C. Law, J. Liu, K. Wang, J. Liu, Y. Liu, Y. Hu, X. Zhang, M. T. Swihart and P. N. Prasad, *Nat. Nanotechnol.*, 2012, **7**, 453–458.
10 S. Hayashi, M. Ito and H. Kanamori, *Solid State Commun.*, 1982, **44**, 75–79.
11 J. Tauc, R. Grigorovici and A. Vancu, *Phys. Status Solidi*, 1966, **15**, 627–637.
12 D. Carolan, *Prog. Mater. Sci.*, 2017, **90**, 128–158.
13 Z. L. Hu, S. Zhang, C. J. Zhang and G. L. Cui, *Coord. Chem. Rev.*, 2016, **326**, 34–85.
14 L. Zhang, B. G. Zhang, B. C. Pan and C. W. Wang, *Appl. Surf. Sci.*, 2017, **422**, 247–256.
15 S. V. Grayli, A. Ferrone, L. Maiolo, A. De Iacovo, A. Pecora, L. Colace, G. W. Leach and B. Bahreyni, *Sens. Actuators, A*, 2017, **263**, 341–348.
16 W. S. Chen, B. C. Chang and K. L. Chiu, *J. Environ. Chem. Eng.*, 2017, **5**, 5215–5221.
17 J. P. Wright, L. J. Harkness-Brennan, A. J. Boston, D. S. Judson, M. Labiche, P. J. Nolan, R. D. Page, F. Pearce, D. C. Radford, J. Simpson and C. Unsworth, *Nucl. Instrum. Methods Phys. Res., Sect. A*, 2018, **892**, 84–92.
18 Y. Matsuura, *Curr. Appl. Phy.*, 2017, **17**, 1465–1468.
19 J. Biedrzycki, K. Tarnowski and W. Urbańczyk, *Opto-Electron. Rev.*, 2018, **26**, 57–62.
20 D. D. Liu, H. S. Liu, C. H. Jiang, J. Leng, Y. M. Zhang, Z. H. Zhao, K. W. Zhuang, Y. G. Jiang and Y. Q. Ji, *Thin Solid Films*, 2015, **592**, 292–295.
21 Ö. M. Dag, A. Kuperman and G. A. Ozin, *Adv. Mater.*, 1994, **6**, 147–150.
22 C. R. Stoldt, M. A. Haag and B. A. Larsen, *Appl. Phys. Lett.*, 2008, **93**, 43125.
23 R. Gresback, Z. Holman and U. Kortshagen, *Appl. Phys. Lett.*, 2007, **91**, 335.
24 Z. C. Holman and U. R. Kortshagen, *Langmuir*, 2009, **25**, 11883–11889.
25 Z. C. Holman, C. Y. Liu and U. R. Kortshagen, *Nano Lett.*, 2010, **10**, 2661–2666.
26 S. Hayashi, M. Fujii and K. Yamamoto, *Jpn. J. Appl. Phys.*, 1989, **28**, L1464–L1466.
27 Y. Maeda, N. Tsukamoto, Y. Yazawa, Y. Kanemitsu and Y. Masumoto, *Appl. Phys. Lett.*, 1991, **59**, 3168–3170.

28 T. I. Kamins, D. A. A. Ohlberg, R. S. Williams, W. Zhang and S. Y. Chou, *Appl. Phys. Lett.*, 1999, **74**, 1773–1775.

29 G. Kartopu, A. V. Sapelkin, V. A. Karavanskii and R. Turan, *J. Appl. Phys.*, 2008, **103**, 113518.

30 S. Ngiam, K. F. Jensen and K. D. Kolenbrander, *J. Appl. Phys.*, 1994, **76**, 8201–8203.

31 D. Carolan and H. Doyle, *J. Mater. Chem. C*, 2014, **2**, 3562–3568.

32 D. Carolan and H. Doyle, *J. Nanomater.*, 2015, **16**, 1–9.

33 N. Shirahata, *J. Solid State Chem.*, 2014, **214**, 74–78.

34 E. Muthuswamy, A. S. Iskandar, M. M. Amador and S. M. Kauzlarich, *Chem. Mater.*, 2013, **25**, 1416–1422.

35 I. I. Dimitri, J. F. Bondi and R. E. Schaak, *Chem. Mater.*, 2010, **22**, 6103–6108.

36 D. J. Xue, J. J. Wang, Y. Q. Wang, X. Sen, Y. G. Guo and L. J. Wan, *Adv. Mater.*, 2011, **23**, 3704–3707.

37 N. K. Mahenderkar, Y. C. Liu, J. A. Koza and J. A. Switzer, *ACS Nano*, 2014, **8**, 9524–9530.

38 A. Lahiri, S. Z. E. Abedin and F. Endres, *J. Phys. Chem. C*, 2012, **116**, 17739–17745.

39 C. Y. Cummings, P. N. Bartlett, D. Pugh, G. Reid, W. Levason, M. M. Hasan, A. L. Hector, J. Spencer, D. C. Snith and S. Marks, *ChemElectroChem*, 2016, **3**, 726–733.

40 A. Lahiri, A. Willert, S. Z. E. Abedin and F. Endres, *Electrochim. Acta*, 2014, **121**, 154–158.

41 A. Lahiri and F. Endres, *J. Electrochem. Soc.*, 2017, **164**, D597–D612.

42 Q. Feng, W. Zhao and S. Wen, *J. Alloys Compd.*, 2018, **744**, 301–309.

43 A. Sánchez and M. Martín, *J. Cleaner Prod.*, 2018, **178**, 325–342.

44 M. F. Ezzat and I. Dincer, *Appl. Energy*, 2018, **219**, 226–239.

45 K. Sakuragi, K. Igarashi and M. Samejima, *Polym. Degrad. Stab.*, 2018, **148**, 19–25.